J Comp Physiol A (2000) 186: 783–797
DOI 10.1007/s003590000131

ORIGINAL PAPER

J. K. Douglass · N. J. Strausfeld

Optic flow representation in the optic lobes of Diptera: modeling the role of T5 directional tuning properties

Accepted: 18 June 2000 / Published online: 26 August 2000
© Springer-Verlag 2000

Abstract An evolutionarily conserved system of small retinotopic neurons in dipteran insects, called bushy T-cells, provides information about directional motion to large collator neurons in the lobula plate. Physiological and anatomical features of these cells provide the basis for a model that is used to investigate requirements for generating optic flow selectivity in collators while allowing for evolutionary variations. This account focuses on the role of physiological tuning properties of T5 neurons. Various flow fields are defined as inputs to retinotopic arrays of T5 cells, the responses of which are mapped onto collators using innervation matrices that promote selectivity for flow type and position. Properties known or inferred from physiological and anatomical studies of neurons contributing to motion detection are incorporated into the model: broad tuning to local motion direction and the representation of each visual sampling unit by a quartet of small-field T5-like neurons with orthogonal preferred directions. The model predicts hitherto untested response properties of optic flow selective collators, and predicts that selectivity for a given flow field can be highly sensitive to perturbations in physiological properties of the motion detectors.

Key words Optic flow · Bushy T cells · Lobula plate · Computational maps · Distributed representations

Abbreviations *COM* center of motion · *EMD* elementary motion detector · *SFMD* small-field motion detector

J. K. Douglass (✉) · N. J. Strausfeld
Arizona Research Laboratories Division of Neurobiology,
611 Gould-Simpson Bldg.,
University of Arizona,
Tucson, AZ 85721, USA
e-mail: jkd@neurobio.arizona.edu
Tel.: +1-520-621-9668; Fax: +1-520-621-8282

Introduction

Studies of small-field retinotopic neurons have identified a subset of lamina and medullary neurons that are sensitive to the direction of motion, and which supply ganglion-cell-like relays to the lobula plate (Strausfeld and Lee 1991; Douglass and Strausfeld 1995, 1996). This cohort of retinotopic neurons is conserved across the Diptera, as well as in Lepidoptera and Hymenoptera (Strausfeld 1976, 1989; Buschbeck and Strausfeld 1996). In contrast, the organization of their postsynaptic targets in the lobula plate – the wide-field collator neurons – can differ radically among taxa and may be associated with the type of visual behavior typifying that taxon (Buschbeck and Strausfeld 1997). How can the taxonomic stability of peripheral motion detecting pathways be reconciled with variability among collator systems that integrate optic flow information for a variety of behavioral tasks? These tasks include distance estimation (David 1982; Srinivasan et al. 1991), collision detection (Wagner 1982; Holmqvist and Srinivasan 1991; Rind 1996; Judge and Rind 1997), estimation of heading direction (Collett and Land 1975; Farina et al. 1994), course stabilization and oculomotor control (Hassenstein and Reichardt 1956; Götz 1975), and stationary (hovering) flight (Wicklein and Strausfeld 2000).

Optic flow-sensitive visual interneurons have been recorded in a variety of taxa and brain centers including the mammalian vestibulocerebellum (Simpson et al. 1981), primate dorsal MST (Saito et al. 1986; Tanaka and Saito 1989), and avian nucleus rotundus (Wang and Frost 1992; Sun and Frost 1998). Optic flow-sensitive neurons in insects include horizontal motion-sensitive neurons in flies (HS cell; Hausen 1982a, b); looming neurons in orthopterans (Gabbiani et al. 1999), and interneurons and descending neurons of odonate, dipteran and lepidopteran brains (Olberg 1981; Gronenberg and Strausfeld 1990; Borst 1991; Kern 1998). Single-neuron selectivity for complex flows, such as wide-field expanding or rotating patterns, is well documented in vertebrates

(Duffy and Wurtz 1991a, b, 1995; Graziano et al. 1994; Wylie and Frost 1999a, b) but less so in insects. In hovering moths, neurons have been anatomically identified that respond selectively to looming or receding stimuli (Wicklein and Strausfeld 2000). In blowflies, receptive field maps of large, uniquely identifiable collator neurons called vertical (VS) and horizontal (HS) neurons reveal their supply by local preferred motion directions (Krapp and Hengstenberg 1996; Krapp et al. 1998). The maps of local directional preference confirm anatomical observations describing the relationships of VS dendrites to regions of the retinotopic mosaic (Strausfeld and Bassemir 1985), and also relate to the location of the tree in different direction-sensitive layers of the lobula plate (Buchner and Buchner 1984). While several of the collator cells are expected to be selective for rotational fields, to date none of the wide-field collator neurons has been tested with a full range of wide-field flow types or flow positions. Such a technically demanding study would profit from predictions that derive from models of two-dimensional motion detector arrays.

This account uses such a model to address the question of how optic flow selectivity, represented as the ensemble responses of retinotopic neurons that are peripheral to wide-field collator neurons, might be mapped functionally onto collators. The model is based on known features of uniquely identified small-field retinotopic neurons, called bushy T-cells (or T5 cells; Strausfeld 1976; Strausfeld and Lee 1991) that respond to motion direction across small areas of the retina (Douglass and Strausfeld 1995, 1996). These cells send their axons into the lobula plate where their terminals are restricted to one of four major direction-sensitive strata (Buchner and Buchner 1984; Fischbach and Dittrich 1989; Strausfeld and Lee 1991). T5 cells are thought to be presynaptic to collator neurons in these strata (Strausfeld and Lee 1991) and thus to supply them with information about the direction of motion. The population and directional properties of T5-like elements are used here to examine their role in generating optic flow selectivity, and to predict response properties of wide-field collator cells both for future physiological analyses and as a way of interpreting the interspecific variation observed among collator neurons.

In the model, the first processing stage defines physiological tuning properties of small-field T5 cells that are broadly tuned to motion direction, excited by preferred-direction motion and inhibited by the null-direction (Douglass and Strausfeld 1995). Physiological and neuroanatomical studies of T5 cells (reviewed by Douglass and Strausfeld 2000b) indicate that there are four T5 cells in each retinotopic column, and suggest that the preferred directions of the T5 cell quartets are roughly orthogonal. Thus, the entire assembly of quartets across the retinotopic map would provide four arrays of small-field motion detectors with orthogonal preferred directions to the four direction-sensitive strata in the lobula plate. A similar segregation of directional selectivity is found in rabbit retina, provided by four directional classes of ON-OFF ganglion cells (Oyster and Barlow 1967; Amthor and Oyster 1995). The best known segregation into orientation-specific layers is in the primate visual cortex (Hubel and Wiesel 1962).

The second processing stage of the model defines specialized spatial patterns of synaptic outputs from small-field motion detectors (SFMDs) to the dendrites of idealized wide-field collator neurons. These connection patterns are called innervation matrices (see Lewis and Kristan 1998), and in effect represent ensembles of T5 elements. Modeling T5 cells provides the basis for predicting general properties of a variety of wide-field lobula plate tangential neurons that are optic flow-sensitive: these include VS and HS cells, the directional sensitivities of which are quite well documented (Hengstenberg 1982; Hausen 1984; Hausen and Egelhaaf 1989; Douglass and Strausfeld 1996), and a number of other wide-field neurons (Hausen 1993; Strausfeld et al. 1995).

The model focuses first on the role of the SFMD physiological properties, using innervation matrices similar to those proposed for primates (Saito et al. 1986; Tanaka and Saito 1989). A second paper (Douglass and Strausfeld 2000a) examines the effects of alternative innervation matrices on optic flow selectivity, with particular reference to interphyletic variability of collator neuron arrangements as opposed to the evolutionary stability of neural arrangements that compose SFMDs (Buschbeck and Strausfeld 1996, 1997). Together, these results demonstrate how both small-field and wide-field parameters shape optic flow-selective properties, and suggest experiments that will reveal which model configurations best fit the observed organization of pathways that process optic flow.

Materials and methods

A feed-forward network was defined with optic flow fields as inputs, and responses of wide-field collator neurons as outputs. Based on the choice of parameters, a particular type of flow field and its position were defined with respect to the joint receptive fields of four arrays of SFMDs. Responses to this flow field were computed for each SFMD, and the response of the wide-field collator neuron was obtained by pooling selected SFMD outputs. For consistency with the nonspiking intracellular voltages exhibited by many peripheral visual interneurons, model outputs at all levels were defined as analog voltages. For comparisons with spiking neurons, however, these responses can be considered analogous to instantaneous spike frequencies. The source code was written in Turbo Pascal 5.0 (Borland International). Figures were made using Origin 5.0 (Microcal, Northampton, Mass.) and CorelDraw 6.0 and 8.0 (Corel, Ottawa, Ontario).

Stimulus generation

Optic flow fields were defined as pure clockwise rotation, counterclockwise rotation, expansion, and contraction, or as combinations of these. Responses to unidirectional flow were tested to evaluate further the sensitivity of particular model implementations to non-preferred flow types. The direction of the unidirectional

flow was always to the right, which is equivalent to any other direction because of circular symmetries inherent in the model.

Corresponding to the lattice organization of visual sampling points (Beersma et al. 1977) flow fields were defined as a rectilinear spatial array (x_i, y_i) of local motion vectors within the receptive field of a wide-field collator neuron. Local vector amplitude served as a measure of local motion speed projected onto the retina, regardless of the combination of rotatory and translatory motions that gave rise to it. Other properties of small-field motion (e.g., intensity and contrast) were omitted in order to focus on the role of SFMD tuning to local direction and speed. Flow fields were defined within a plane perpendicular to an axis that intersects the center of a collator neuron's receptive field. Centered flow fields (e.g., Fig. 1A) correspond to self-motion along a collator axis (pure expansion or contraction), rotation about the axis (pure clockwise or counterclockwise rotation), or combinations of these. Non-centered flows, such as the rotatory flow illustrated in Fig. 1B, correspond to the same kinds of motion but with the center of motion (COM) displaced.

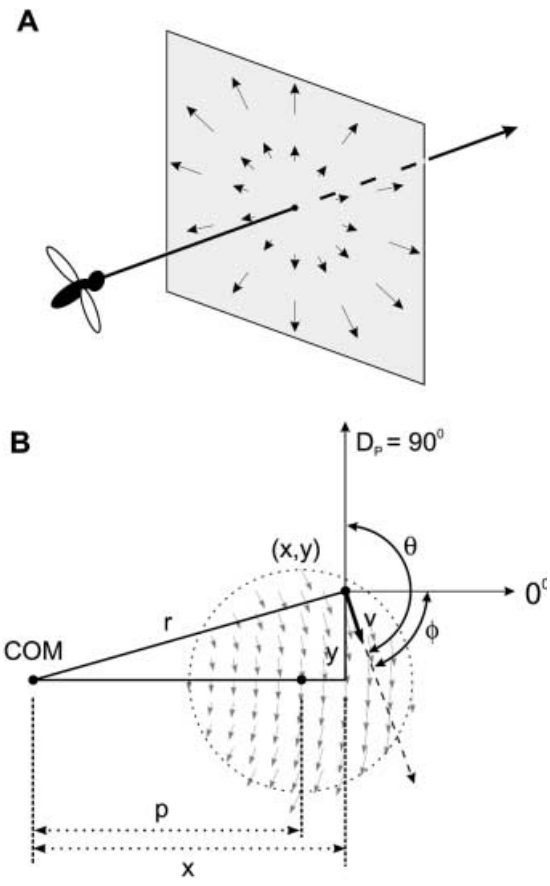

Fig. 1A, B Optic flow patterns and the method used to compute local motion vectors. **A** An expanding flow field resulting from forward motion along the *z*-axis is centered on the receptive field of a collator neuron that has a frontal field of view, and is off-center for neurons serving other fields of view. **B** An example of clockwise rotatory flow, here with its center of motion (COM) positioned two radii leftward from the center of a collator neuron's receptive field (*dotted circle*). Thus, in relative units of stimulus position employed throughout this paper, the stimulus position (p) equals −2. Directions and magnitudes of local motion vectors (*lightly shaded arrows*) were computed at all locations (x, y) of small-field motion detectors (SFMDs) within the collator receptive field based on the type of flow field, the SFMD position with respect to the COM, and angles corresponding to preferred directions (D_P) of the SFMDs (see Materials and methods, Eqs. 1 and 2). For vector v the absolute direction ϕ is approximately −75°, and its direction θ relative to a D_P of 90° is approximately −165°

The absolute direction (ϕ) of each local motion vector v was computed according to the type of flow field and the Cartesian coordinates of the vector with respect to the COM (Fig. 1B):

$$\begin{aligned} \phi &= \sin^{-1}(y/r) + c, x > 0 \\ \phi &= 180 - \sin^{-1}(y/r) + c, x \leq 0 \end{aligned} \tag{1}$$

The arcsine term provides the angle of a radius (r) from the COM to the location (x, y) of an SFMD, and the constant (c) determines the type of flow field by adjusting the local motion direction with respect to the radius (for example, $c = -90°$ for pure clockwise rotation, 0° for expansion, 90° for counterclockwise rotation, and 180° for contraction). In order to compute responses of SFMDs to motion, the local motion direction (θ) was computed relative to the preferred direction (D_p) of an individual SFMD, with D_p defined as the local motion direction that produces the maximum positive response amplitude:

$$\theta = \phi - D_p \tag{2}$$

To facilitate future comparisons with physiological data and comparisons among responses to different flow types, several model parameters are defined in relative instead of absolute units. Thus, the distances x and y are defined relative to a collator with a unit receptive field radius of 1. To a first approximation, the planar flow patterns defined in the model are similar to stimuli that are used during intracellular recordings and serve to approximate inputs to collators having a range of absolute receptive field sizes approaching a hemispherical panorama. Except for tests of model output as a function of flow speed, the overall flow speed (corresponding to rotations per minute for pure rotational flow, or m/s for pure expansion) was kept fixed at a value that maximized the overall model output during centered flow.

Small-field motion detector responses

The model SFMDs simulate responses of T5 cells as a function of the local angular speed (S) and direction (θ) of a contrasting edge. Because responses of T5 cells as a function of motion speed have yet to be tested, the model assumes a generic speed response function (Fig. 2A):

$$F(S) = k \cdot S \cdot e^{(1-k \cdot S)} \ , \tag{3}$$

which is qualitatively similar to the Gaussian functions employed by Perrone (1992) and provides a good match to current physiological data on motion speed and/or contrast frequency from a variety of directionally selective visual interneurons (rabbit ON-OFF direction sensitive ganglion cells: Wyatt and Daw 1975; fly lobula plate tangential cells: Hausen 1982a, b; single-units in macaque area MT: Maunsell and Van Essen 1983). The value of k sets the speed response maximum at a speed of $1/k$, and was arbitrarily fixed at a value (1.79), which maximized the sum of the SFMD responses within a unit collator receptive field radius during centered flow.

The directional tuning of the SFMDs was specified by one of four alternative cosine-shaped directional response functions (Fig. 2B–E) chosen to encompass a broad range of possible tuning characteristics for T5 cells (see Discussion) and normalized to a peak-to-peak amplitude of 1.0. These alternative functions (Eq. 4) are either broadly [$G_A(\theta)$, $G_B(\theta)$], or narrowly [$G_C(\theta)$, $G_D(\theta)$] tuned to the local relative motion direction θ (from Eq. 2), and produce either purely excitatory [$G_A(\theta)$, $G_C(\theta)$], or combined excitatory and inhibitory [$G_B(\theta)$, $G_D(\theta)$] responses:

$$\begin{aligned} G(\theta) &= b + 0.5 \cdot \cos(a \cdot \theta), |\theta| < 180°/a, \\ G(\theta) &= b - 0.5, |\theta| \geq 180°/a, \end{aligned} \tag{4}$$

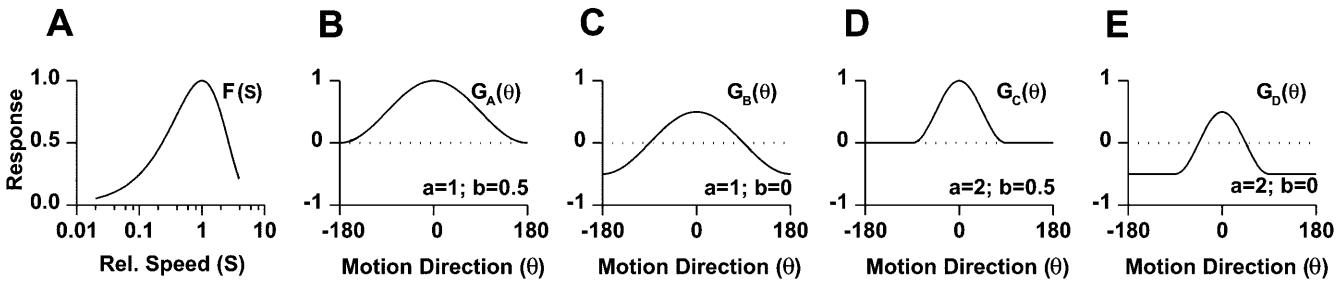

Fig. 2A–E Speed and direction tuning functions used to define response properties of four configurations of small-field motion detectors. **A** Speed tuning function (Eq. 3), with responses normalized to the speed response maximum. **B–E** Alternative directional tuning functions (G_A, G_B, G_C and G_D, respectively), defined by using Eq. 4 with the values shown for the broadness (a) and offset (b) parameters

where b specifies a constant offset from the zero response level, and a determines the broadness of directional tuning. The overall response of each SFMD was computed by combining Eqs. 3 and 4 to give:

$$R(\theta,S) = (b + 0.5 \cdot \cos(a \cdot \theta)) \cdot k \cdot S \cdot e^{(1-k \cdot S)}, |\theta| < 180^\circ/a$$
$$R(\theta,S) = (b - 0.5) \cdot k \cdot S \cdot e^{(1-k \cdot S)}, |\theta| \geq 180^\circ/a. \quad (5)$$

The assumption that a purely analytical model such as Eq. 5 can adequately represent the responses of an SFMD has a precedent in primate-inspired models (Perrone 1992; Perrone and Stone 1994, 1998). To further evaluate the suitability of Eq. 5 to insect motion processing, its properties were compared with two versions of a Hassenstein-Reichardt correlation-type elementary motion detector model with asymmetrical delays and a multiplicative interaction between two input channels (Hassenstein and Reichardt 1956; Borst and Egelhaaf 1989). The basic configuration (Fig. 3A) employs a standard "mirror-symmetrical" design that is supported by physiological studies of wide-field tangential neurons, in particular the H1 and HS neurons of blowflies (Franceschini et al. 1989; Borst and Egelhaaf 1990; Brotz and Borst 1996). Briefly, the inputs were defined as moving ON or OFF edges which produced analog ON and OFF voltage responses at each input channel, like intracellular responses of fly lamina monopolar cells L1-L5 (e.g., Laughlin 1981; Gilbert et al. 1991; Douglass and Strausfeld 1995). The speed optimum for this elementary motion detector (EMD) circuit is determined mainly by the ratio of the angular separation between channels and the internal delay D (here set at 2° and 12 ms, respectively) and to a lesser extent by the kinetics of the single-channel ON and OFF responses prior to the multiplication stage. Outputs from two elementary motion detectors with opposite preferred directions were subtracted to yield an SFMD with excitatory responses to preferred-direction motion and inhibitory responses to null-direction motion, consistent with the responses of T5 cells (Douglass and Strausfeld 1995). SFMD responses to a full 360° range of motion directions were computed by adjusting the delay between the activation by a moving edge of one input channel

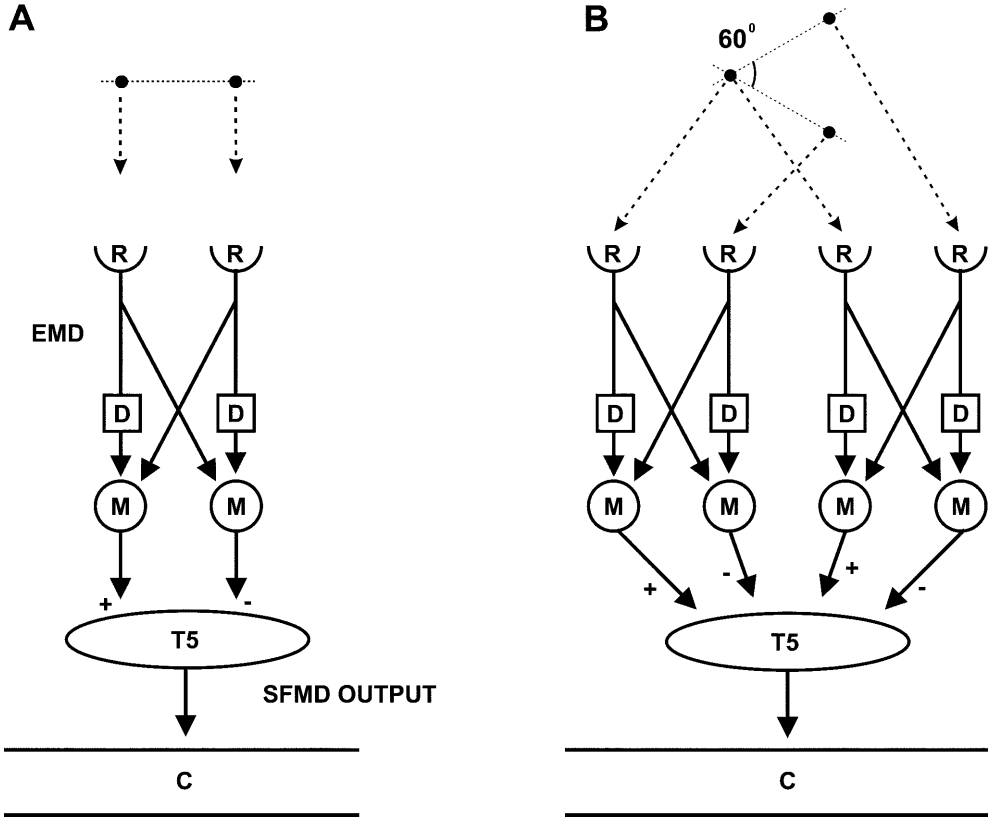

Fig. 3A, B The identification of small-field, motion-sensitive neurons supports a modified correlation-type model of small-field directionally selective motion detector (SFMD) circuits. The filled circles (*top*) represent adjacent retinotopic channels that provide light-sensitive inputs (R) to one (**A**) or two (**B**) mirror-symmetrical motion detector circuits. **A** Essentials of this circuit are compatible with the two-channel mirror-symmetric elementary motion detector (EMD) equipped with a fixed internal delay (D), a multiplicative interaction (M) between the responses of each channel, and a subtraction stage. **B** A three-channel model comprises a duplication of mirror-symmetry within the retinotopic map along two axes diverging by 60°, in accordance with optomotor experiments and retinal maps of visual sampling points (Buchner 1976; Beersma et al. 1977). See Materials and methods for details

and the next. For preferred-direction (0°) or null-direction (180°) motion, this delay is simply the angular separation $\Delta\phi$ between the two input channels, divided by the motion speed S (°/s). As the motion direction θ departs from the preferred direction (0°), the delay diminishes as the cosine of θ. Thus, the overall delay $D = \cos(\theta) \cdot \Delta\delta\phi/S$.

An alternative correlation-type model was tested to illustrate response properties of a slightly more spatially distributed circuit. This configuration (Fig. 3B), which is supported by optomotor experiments on *Drosophila* (Buchner 1976), has three input channels supplying two pairs of mirror-symmetrical EMDs. The preferred/null axes of the EMDs were separated by 60° (corresponding to the hexagonal ommatidial lattice of the fly compound eye), and the outputs of the two subcircuits were summed.

Wide-field collator organization

The second processing stage specifies the retinotopic organization of four superimposed arrays of model SFMDs and their patterns of output connections to wide-field collator neurons (Fig. 4). SFMDs within each array comprise a rectilinear array within a circular field defined as coinciding with the collator receptive field. Each SFMD array was arbitrarily defined to contain 73 SFMDs with a maximum of 292 outputs from the four arrays. The number of SFMDs per array was increased to 701 in tests where the results are presented as contour plots of spatial activity patterns (see below) in order to obtain smooth contour lines. The salient features of the model responses apply equally well to other array densities (see Buchner 1976) except that spatial sampling biases can distort the responses at very low SFMD densities.

To conform to the organization of four directionally selective T5 neurons per column (Douglass and Strausfeld 2000b), all of the SFMDs within an array shared the same preferred direction (D_P). The D_Ps of the four arrays were to upward, downward, rightward and leftward motion (Fig. 4B). For each SFMD array, an innervation matrix was designed to produce selectivity for a particular optic flow type by specifying excitatory output connections from all SFMDs that occupy a restricted region of the retinotopic map, and no connection for SFMDs in other regions (Fig. 4C). This quadripartite arrangement is similar to those proposed for optic flow processing in primate MSTd (Saito et al. 1986) and corresponds to patterns of dendritic stratification of wide-field tangential neurons in four functional layers of the lobula plate (Buchner and Buchner 1984). The example in Fig. 4C shows innervation matrices designed to produce selectivity for clockwise rotation. Output connections from the rightward-sensitive SFMD array ($D_P = 0°$) are restricted to the upper quadrant (shaded), those from the upward-sensitive array are from the left quadrant, and so on. Equivalent innervation matrices selecting for counterclockwise rotation, expansion or contraction were specified by shifting the polar coordinates of the output regions by 180°, –90°, or +90°, respectively. Patterns for non-cardinal flow types were generated using intermediate shifts. The patterns of output connections always occupied a radial bandwidth of 90°, and all nonzero synaptic weights had a value of 1.

Model outputs

The overall output from the second processing stage represents responses of a wide-field collator neuron to optic flow fields. These responses were obtained as the linear sum of responses from those SFMDs provided with output connections (Fig. 4D), and always employed stimulation of the full receptive field of the collator. Concerted "population activity" of arrays of SFMDs was also examined, by using contour plots computed from the arrays of individual response strengths. These spatial activity patterns were examined both at the level of raw "presynaptic" SFMD responses

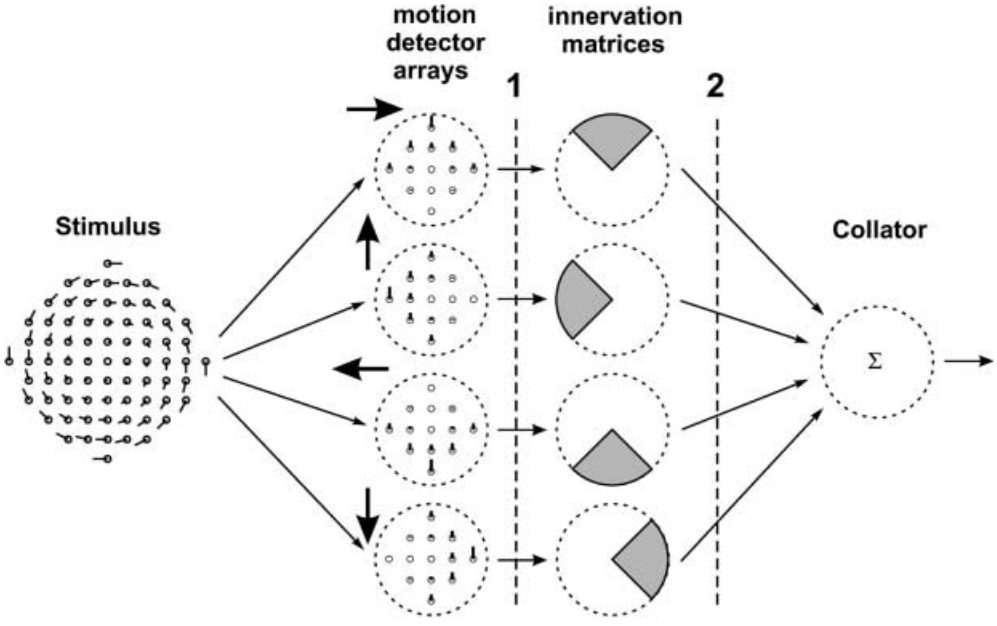

Fig. 4 Overall architecture of the optic flow processing network. The optic flow stimulus is here depicted as a clockwise rotational flow that is centered on the receptive field (*dotted circles*) of the collator, and provides inputs to four superimposed arrays of SFMDs. The arrays have orthogonal preferred directions to upward, downward, leftward and rightward motion (*large arrows*), and the individual response amplitudes (*vertical lines* at each SFMD location) are a function of local motion direction and speed (see Eq. 5). This example illustrates responses of SFMDs with directional tuning properties described by function R_A. The synaptic innervation matrices, in this case designed to promote selectivity for clockwise flow, transfer SFMD responses from the shaded regions for linear summation by a wide-field collator neuron. Other innervation matrix positions can be used to generate selectivity for other flow types. For clarity of presentation, only 13 SFMDs per array are illustrated. Actual model computations used either 73 SFMDs per array, or 701 for contour plots of spatial activity patterns (see Materials and methods). *Dotted vertical lines* (1 and 2) indicate processing levels that correspond to the spatial activity patterns illustrated in Figs. 7 and 8

(Fig. 4, dotted line 1), and as "postsynaptic" voltages within the dendrites of a collator, before summation (Fig. 4, dotted line 2).

Results

Properties of small field motion detector models

Figure 5 shows overall response profiles of an individual SFMD as a function of motion direction and speed. With the motion direction fixed at 0°, the analytical models (Fig. 5A–D) and correlation models (Fig. 5E, F) exhibit similar tuning to motion speed (Fig. 5): consistent with Eq. 3 (see Materials and methods) as well as previous observations on correlation-type models (e.g., Zaagman et al. 1978), there is a single response peak, with a sharp decrease in response amplitudes at lower speeds and gradually diminishing responses at higher speeds. Responses to other motion directions are more complex. For the analytical SFMD models (Fig. 5A–D),

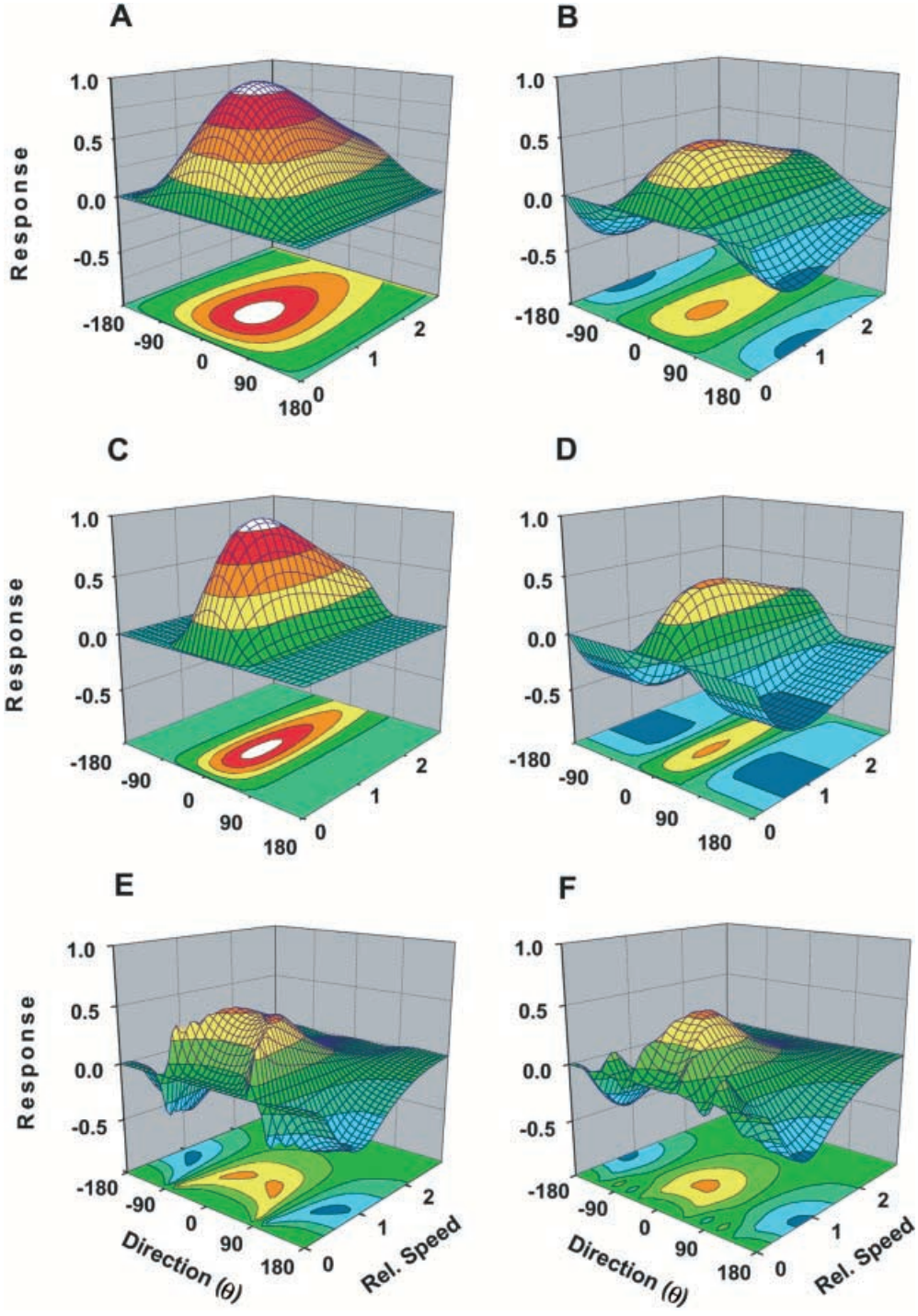

Fig. 5 Comparison of responses to local motion direction and speed by the four alternative analytical SFMD models (**A–D**; defined in Eq. 5) and two correlation-type SFMD models (**E**, 2-channel model; **F**, 3-channel model). Responses are normalized to a peak-to-peak amplitude of 1, and motion speeds are normalized to the speed that evoked maximal responses. In the correlation-type models, the response maximum is determined by the internal delay and the kinetics of the single-channel ON and OFF responses prior to the multiplication stage. The more spatially distributed 3-channel version (**F**) produces a less complex response profile that is qualitatively similar to the analytical SFMD models, thus supporting the biological plausibility of the latter

responses reflect the combined effects of the speed tuning and the individual directional tuning functions, and differ, as intended, only with regard to the broadness of the directional tuning and the presence or absence of inhibitory responses. The two-channel correlation model (Fig. 5E), however, shows no single optimal combination of preferred speed and direction. Instead, two response peaks occur at about +30° and −30°, and at slower speeds, the directional tuning is strongly speed-dependent. The inhibitory responses (at motion directions beyond ±90°) are symmetrical with the excitatory responses, with two inhibitory maxima at approximately +150° and −150°. The complexity in this response profile arises mainly because the temporal delay in edge arrivals at the two input channels depends on both the speed and direction of motion. Related phenomena have been discussed with reference to the sensitivity of wide-field neurons to the contrast frequency of periodic gratings moving along the preferred-null axis (Zanker 1990).

Viewed in isolation, the results from the two-channel correlation model seem to suggest that the analytical models are oversimplified. However, the slightly more spatially distributed three-channel correlation model (Fig. 5F) shows far less complexity in its response profile. Except for small peaks at the slowest motion speeds, the three-channel model exhibits one major response maximum and minimum, and its overall shape is similar to that of analytical function R_B (Fig. 5B). T5 cells appear to receive inputs from as many as seven neighboring retinotopic columns (Strausfeld and Lee 1991), so the three-channel SFMD model is conservative with regard to the distributed nature of inputs. Meanwhile, the directional selectivity of an R_B-like SFMD could easily be sharpened (R_C- or R_D-like) by the presence of lateral inhibitory connections among neighboring SFMDs, and the inhibitory response components could be reduced (R_A-like) by various modulatory effects on membrane potential. Thus, the four analytical models all specify plausible alternative response properties for T5 cells.

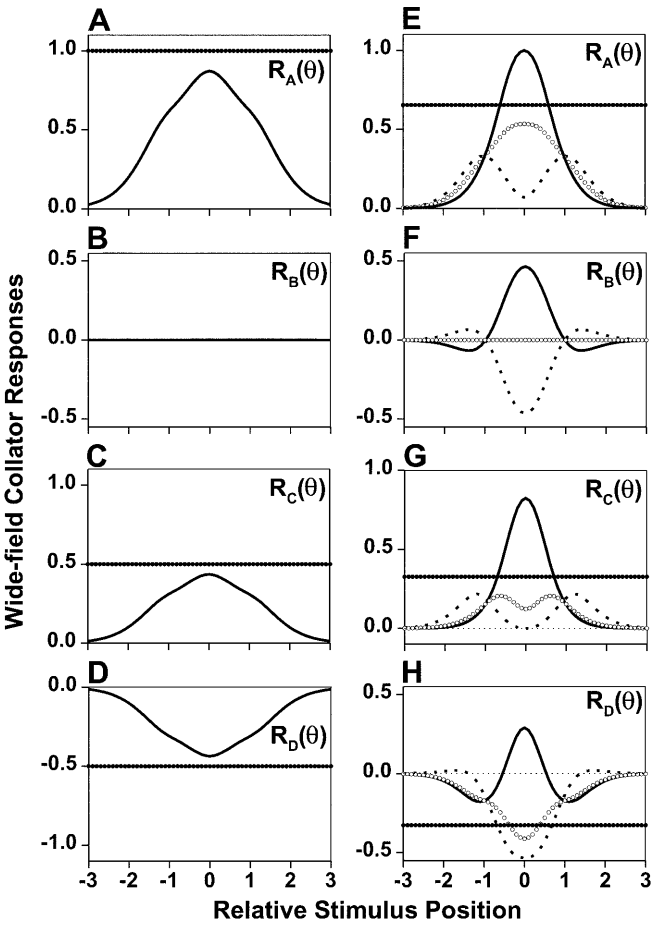

Fig. 6 Collator responses to various optic flow inputs in networks endowed with one of the four alternative small-field directional tuning functions [**A, E** $R_A(\theta)$; **B, F** $R_B(\theta)$; **C, G** $R_C(\theta)$; and **D, H** $R_D(\theta)$], and using either a 1–1 innervation matrix (**A–D**) or a matrix designed to promote selectivity for clockwise rotation (**E–H**). Data are plotted as a function of the position of the center of motion (*relative stimulus position*) in units of collator receptive field radii, and are normalized to the maximum response observed from all four directional tuning functions. **A–H** show responses to clockwise rotation (*solid curves*) and unidirectional flow (*dotted*). With the one-to-one matrix (**A–D**), responses to counterclockwise rotation, expansion and contraction were identical to those for clockwise rotation. With the "clockwise rotation" matrix, **E–H** show distinct responses to counterclockwise rotation (*dashed*), and identical responses to expansion and contraction (*open circles*). Note that for **E–H**, symmetrical results were obtained by specifying innervation matrices that are selective for other optic flow types (see Results)

Raw SFMD responses produce selectivity for flow position, but not flow type

Figure 6 compares the responses of a wide-field collator to five cardinal optic flow field types and across a range of flow-field positions, using each of the four alternative analytical SFMDs. Figure 6A–D illustrates the outputs from a network that lacks any specialized innervation matrix. Instead, the SFMDs in each array were provided with one-to-one output connections to the collator, equivalent to a uniform innervation matrix with a 360° bandwidth. With this very simple configuration, three of the four SFMD tuning functions result in some selectivity for optic flow *position*, with the response maximum (Fig. 6A, C) or minimum (Fig. 6D) corresponding to centered flow. There is no flow *type* selectivity, however, except that unidirectional flow produces position-invariant responses. Thus, for each of the alternative SFMD types, the responses to clockwise rotation, counterclockwise rotation, expansion and contraction (*solid lines*) are all identical.

Simple innervation matrices produce selectivity to flow type but sensitivity to small-field tuning

Figure 6E–H shows responses to various flow types and positions as in Figure 6A–D, but now using a special-

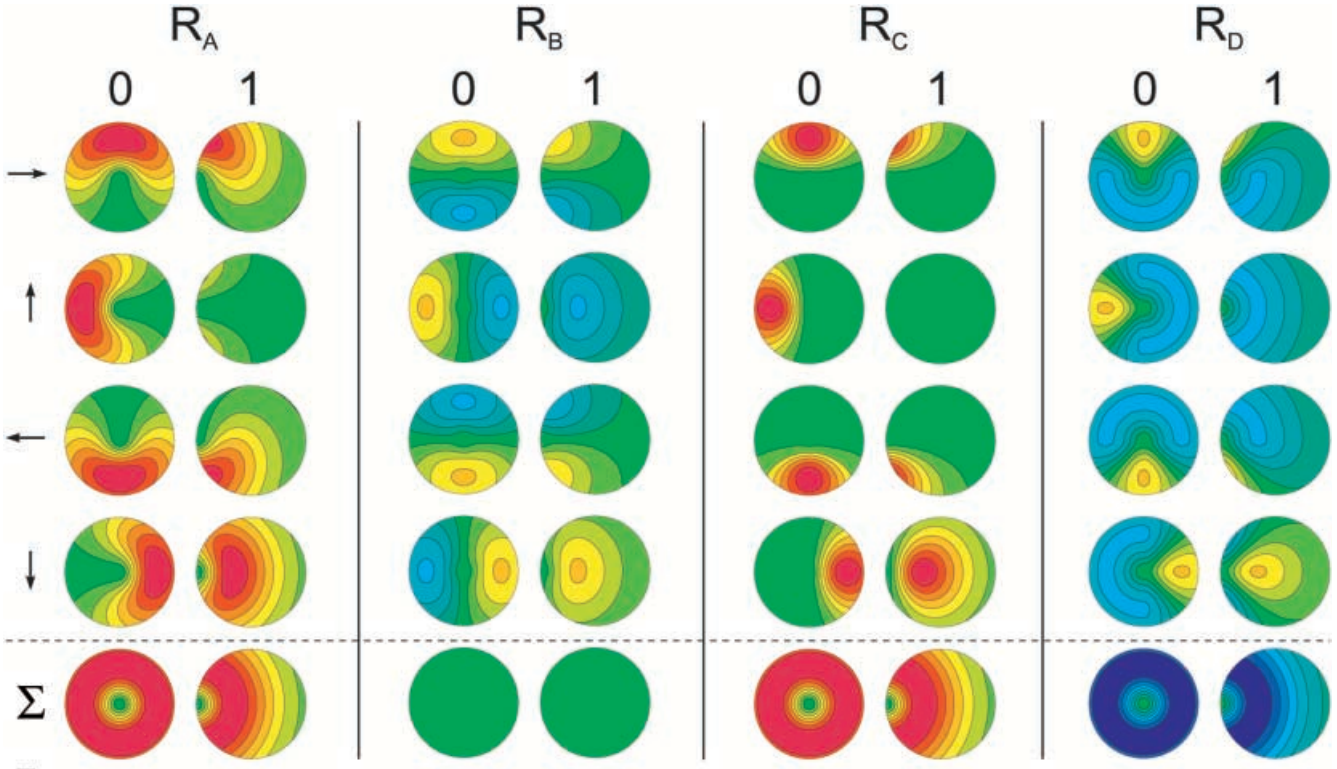

7

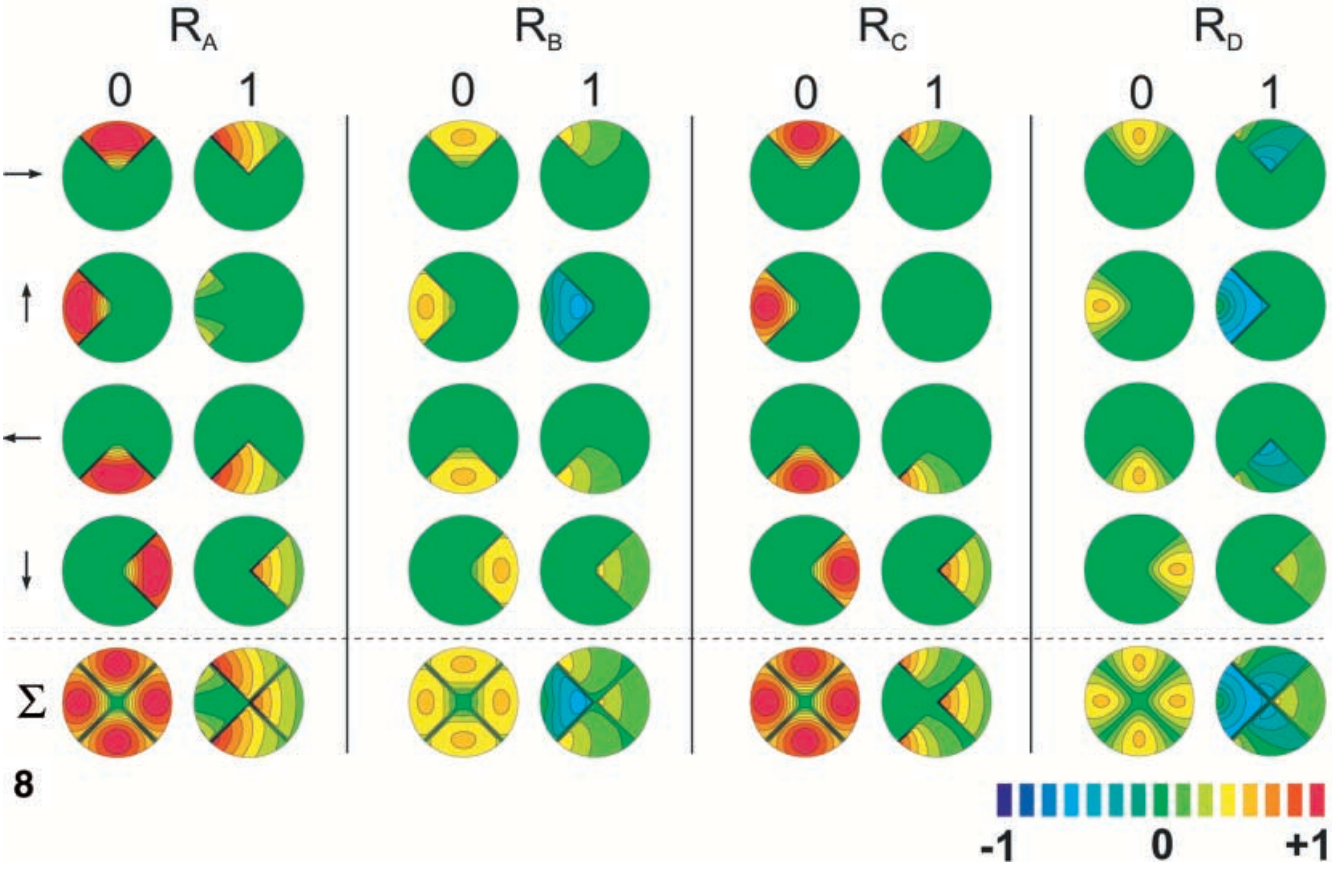

8

◀

Fig. 7 Predicted "presynaptic" population activity of SFMDs, corresponding to level 1 in Fig. 4 and shown as contour plots of response amplitudes ranging from strongly excitatory (red) to strongly inhibitory (blue). The color code is normalized to the maximum and minimum summed response amplitudes. Responses to pure clockwise rotation were calculated for the four arrays of SFMDs endowed with orthogonal preferred directions (*arrows at left*), then spatially summed (Σ). Responses are shown for the four alternative small-field directional tuning functions (R_A, R_B, R_C and R_D, respectively) during centered flow (position *0*) and flow positioned at the edge of the collator receptive field (position *1*)

Fig. 8 Predicted "postsynaptic" population responses to clockwise rotation, in a network with an innervation matrix designed to promote selection for clockwise rotation. The data correspond to level 2 in Fig. 4, and are plotted and color-coded as in Fig. 7. The summed data (Σ) predict the spatial pattern of dendritic activity in a collator that is selective for centered, clockwise rotatory flow. Note that the quadrimodal patterns in summed response amplitudes reflect both the arrangement of the innervation matrices and the quadrimodal distribution of SFMD preferred directions. Thus, in principle, information about these network characteristics can be deduced experimentally during stimulation with optic flow patterns (see Discussion)

ized innervation matrix designed to promote selectivity for clockwise rotation. In contrast with the one-to-one mapping results, responses to clockwise rotation (*solid line*), counterclockwise rotation (*dashed line*), expansion/contraction (*open circles*) and unidirectional flow (*dotted line*) are now distinct: Each SFMD tuning function now produces position selectivity to two or more of the cardinal flow types. More importantly, all four small-field tuning functions produce some degree of flow *type* selectivity. R_B (Fig. 6F) clearly provides the most effective overall selectivity for clockwise rotation, with strong, position-sensitive responses to clockwise rotation, symmetrical inhibitory responses to counterclockwise flow, and complete insensitivity to the other cardinal types. The selectivity of the other three small-field functions (Fig. 6E, G, H) is compromised by strong responses to unidirectional flow and complex responses to other flow types. Moreover, R_B produces a lateral-inhibition-like effect on the responses to rotational flows centered just beyond the edge of the collator receptive field. In a higher-level network that compares responses of several flow detectors with overlapping receptive fields, this center-surround effect could enhance the ability to discriminate flow field position.

These results demonstrate that excellent selectivity for clockwise rotation can be obtained using a simple, uniform innervation matrix designed for sensitivity to this flow type. In other tests (not shown), analogous uniform mappings designed to produce selectivity for counterclockwise rotation, expansion, and contraction produced results identical to those in Fig. 6E–H, except that selectivity was shifted to the newly defined preferred type, and away from the respective orthogonal flow types. For example, when the small-field tuning function R_B was combined with an innervation matrix designed to detect pure expansion, the responses to centered expansion were excitatory (Fig. 6F, *solid line*), those to contraction were inhibitory (Fig. 6F, *dashed line*), and there was no response to either clockwise rotation, counterclockwise rotation or unidirectional flow. Innervation matrices can be adjusted in the same manner to maximize responses to any flow type that is intermediate between expansion, contraction and rotation, simply by shifting the polar coordinates of those retinotopic regions endowed with output connections.

Spatial activity patterns reveal mechanisms of flow processing

Many of the mechanisms that produced the summed collator outputs in Fig. 6 are revealed by examining spatial patterns of SFMD activity predicted by the model at earlier processing levels. Only responses to clockwise rotation are illustrated here. Figure 7 shows the predicted "presynaptic activity" of each SFMD array during clockwise rotation (see Fig. 4, processing level 1), and Fig. 8 shows the resultant "postsynaptic" activity after filtering by the clockwise rotation innervation matrix (Fig. 4, level 2).

The raw SFMD activity in Fig. 7 illustrates the interaction of spatially mapped local motion vectors with the small-field (non-mapped) directional- and speed-tuning properties of SFMDs. Different local activation levels result from the distinct preferred directions of the SFMD arrays, and from differences in excitatory and inhibitory responses associated with the four SFMD tuning functions. Each SFMD tuning function produces maximal excitatory activity (red and orange contours) in areas where the local flow corresponds to the most preferred combination of direction and speed, and inhibitory activity (R_B and R_D, blue contours) where the directional tuning includes inhibitory responses and the local motion is in a non-preferred direction. During centered flow (Fig. 7, position 0), the spatial activity patterns within individual columns of SFMD arrays are identical except for their orientations, which differ according to the preferred directions of the arrays. This generalization applies to all flow types defined by Eq. 1, and helps explain the lack of flow *type* selectivity in the absence of a specialized innervation matrix (Fig. 6A–D). The reason flow *position* selectivity is already present at this processing level is that the response patterns among the four SFMD arrays are identical only for centered flow. Displacement of the flow from the receptive field center (e.g., Fig. 7, position 1) shifts the response pattern of each SFMD array laterally, bringing different portions of the underlying pattern into the collator receptive field.

The postsynaptic spatial activity patterns (Fig. 8) demonstrate how the addition of specialized innervation matrices permits four very different directional

tuning functions to produce excitatory, position-dependent responses to clockwise rotation (Fig. 6E–H). Despite considerable differences among the presynaptic patterns associated with a given preferred direction (Fig. 7), all four functions produce maximal excitation within the same spatial regions of the retinotopic map. The innervation matrices for clockwise rotation select responses from precisely these regions (Fig. 8, position 0), and exclude other regions where the response patterns differ the most. This example demonstrates how specific computational properties (here, selectivity for clockwise flow) arise from the interaction of small-field, nonspatial properties with a spatially mapped neuropil.

Robustness of optic flow selectivity at different motion speeds

Small-field tuning function R_B produces strong selectivity for flow type and position when the optic flow speed has been pre-set to maximize the sum of the SFMD responses within the collator receptive field (Fig. 6F). Is this selectivity maintained at other optic flow speeds? Tests using clockwise rotation (Fig. 9A) as well as other flow types confirmed that position selectivity remains intact over a broad range of speeds. Meanwhile, sensitivity to non-preferred flow types remains low, as illustrated in Fig. 9B by the responses of a "clockwise rotation detector" to expansion, contraction and unidirectional flow. With the preferred flow (Fig. 9A), the peak response amplitude consistently occurs when the flow is centered on the collator's receptive field, except at the very slowest speeds, where the maximum responses occur at increasing distances from the receptive field center. This effect can be explained as follows. With slow, centered rotatory flow, the local motion speed at each SFMD is too slow to generate strong responses, even though local flow directions are well aligned with preferred directions of precisely those SFMDs that have output connections. With increasingly off-centered flow, the local directions become more unidirectional and the local flow speeds increase (see Fig. 1B). Fewer SFMDs with output connections receive preferred-direction inputs, but because those SFMDs are also located where the local speeds are high, they can produce a stronger collated response. The predicted shift in the preferred flow position at the slowest flow rates has yet to be tested in recordings from optic flow-selective neurons.

Coarse coding for optic flow type and position

A widespread feature of many neuronal information processing systems is that their individual elements often are broadly tuned (coarsely coded) to simple input parameters (Heiligenberg 1987; Sparks et al. 1997). How broadly tuned is this model to flow field speed, position and type? Figure 9 demonstrates broad tuning to flow speed, in a manner that clearly is controlled by the shape of the small-field speed response function.

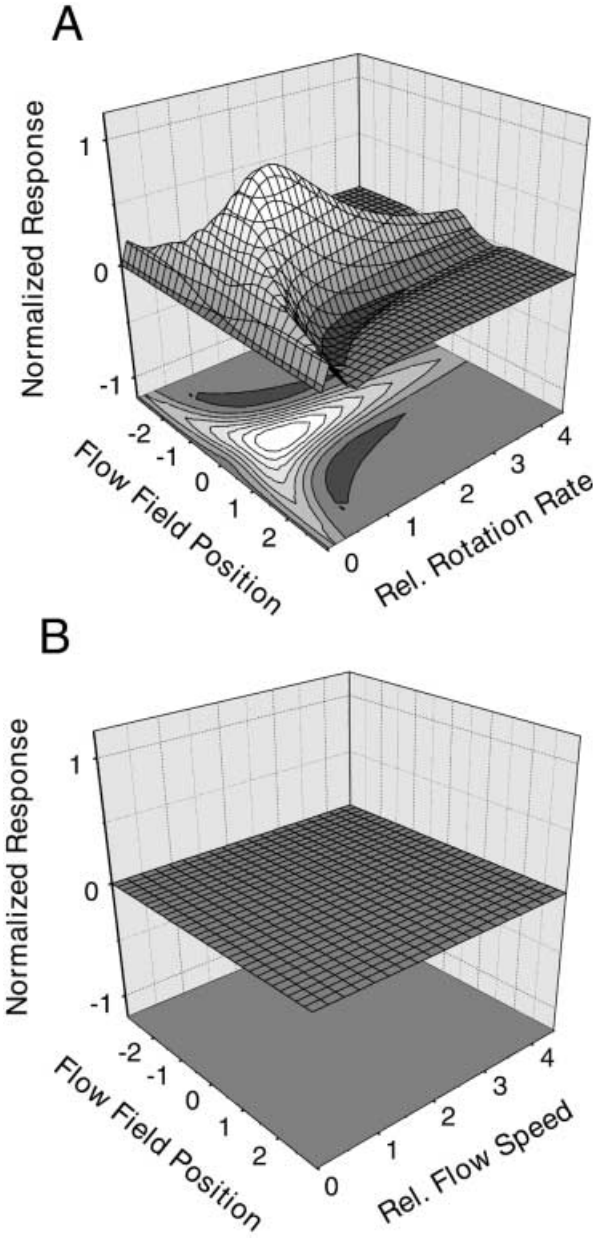

Fig. 9A, B Speed tuning of an optic flow processing network, implemented using small-field tuning function R_B and innervation matrices designed to promote selectivity for clockwise rotation. **A** Responses to clockwise rotation, plotted as a function of *flow field position* (in collator receptive field radii) and *rotation rate*, plotted relative to the rotation rate at which maximal responses occur. **B** The zero responses to expansion, contraction, and unidirectional flow, demonstrated for a single flow speed in Fig. 6F, persist at all flow speeds and positions

The network is also broadly tuned to flow field position. For example, with directional tuning function R_B, responses to the preferred flow type are maximal to

centered flows and diminish gradually as the COM moves beyond the receptive field edge (Fig. 6F). Responses to flow field type are also coarsely coded. This was demonstrated by varying the flow type parameter c in Eq. 1 between −180° and 180° (see Materials and methods). As Figure 10A shows for an innervation matrix designed to produce selectivity for pure expansion, the flow type tuning has a half-bandwidth of 180°, and precisely fits a cosine function. The coarse overall tuning to flow type and position (Fig. 10B) illustrates the variety of inputs to which an individual collator will respond. At a subsequent processing level, the concerted activity of only a few differently-tuned collators can provide the basis for fine discriminations among these inputs.

Discussion

Comparisons with other models for flow-field analysis

A feed-forward, retinotopic and optic flow-selective network has been derived from structural and functional features of small field directional motion-sensitive neurons and their synaptic outputs to lobula plate collators. The network has determined basic requirements for generating collators tuned to both the type and position of optic flow. Optic flow selectivity is highest when SFMD tuning properties are specified by the function (R_B), with broad directional tuning and incorporating both excitatory and inhibitory responses. The positions of innervation matrices can be adjusted so as to generate a wide variety of flow type selectivities, all by using the same set of raw responses from the four SFMD arrays. The optic flow selectivity is also robust to changes in flow speed.

Numerous models have been proposed to explain how optic flow processing networks can provide information on heading (Perrone 1992; Lappe and Rauschecker 1993) and time-to-collision (Rind and Bramwell 1996), or contribute to higher-level analyses of three dimensional structure (reviews by Nakayama 1985; Koenderink 1986; Cornilleau-Pérès and Gielen 1996). The present model is concerned with basic mechanisms that generate selectivity for optic flow type and position in single neurons, and conforms to the characteristics and limitations of visual processing pathways in Diptera. These mechanisms are consistent with the "direction mosaic hypothesis" (Duffy and Wurtz 1991b) in which arrays of small-receptive-field elements sensitive to local motion direction have outputs arranged to yield selectivity for a particular flow pattern by a wide-field collator neuron.

The forms of tuning curves for flow type and position predicted by the present model are similar to responses of vertebrate neurons that are tuned to optic flow type and position, and to the tuning properties of a direction mosaic model of optic flow processing in primate cortex (Perrone 1992; Perrone and Stone 1994, 1998). For example, the model's coarse tuning to flow type (cf. Fig. 10) is virtually identical to the cosine-like flow type tuning in macaque MSTd (Graziano et al. 1994; Duffy and Wurtz 1995), and the predicted broad tuning to flow position is consistent with physiological recordings from visual areas in the avian brain that process translational and rotational flows (Wylie and Frost 1999a, b). With few exceptions (Wicklein and Strausfeld 2000), direct evidence for selectivity to complex optic flow fields (as opposed to looming objects) in insect wide-field neurons comes from experiments that employed relatively simple patterns composed of one to two unidirectional gratings. Thus, to test predictions of this model it will be neces-

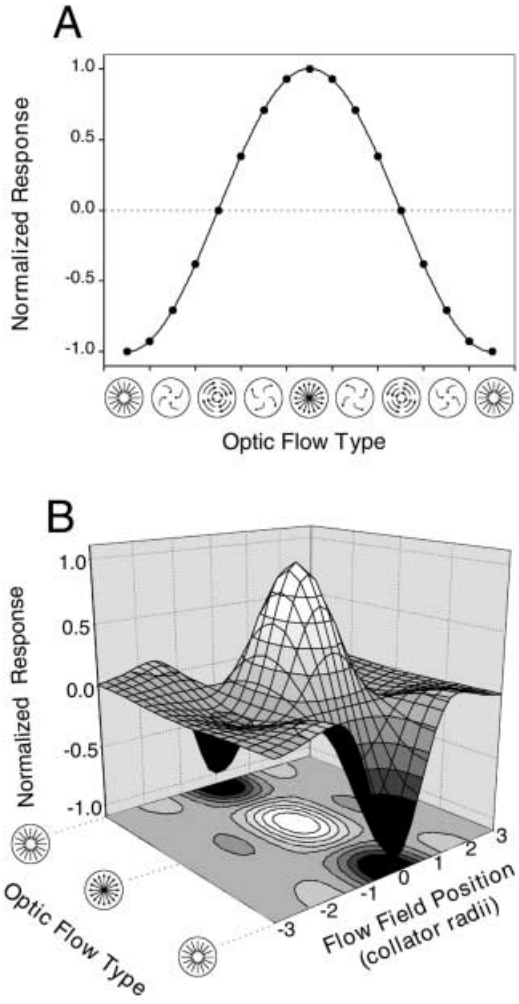

Fig. 10A, B Coarse coding of the model's responses to optic flow position and type. Responses are normalized to the maximum. **A** Responses to different flow types by an R_B-based network with an innervation matrix designed to promote selectivity for a centered, pure expanding flow. The continuum of flow types (*abscissa*) corresponds to an angular scale determined by the value of parameter c in Eq. 1, with pure expansion at $c = 0°$ and pure contraction at $c = \pm 180°$. With this transformation, the responses (*dots*) closely fit a cosine function (*solid curve*) with a half-bandwidth of 180°. **B** Responses of the same network implementation as in **A**, now shown as a function of both optic flow type and flow field position (cf. Fig. 6F)

sary to record physiological responses to the full range of complex optic flow types and positions.

How many small-field directional classes are sufficient to analyze optic flow?

A basic assumption of the present model is that the distribution of preferred directions among small-field motion detectors is tightly clustered into four orthogonal groups, a feature that is well-known in the ON-OFF direction-sensitive ganglion cells of the rabbit retina (Oyster and Barlow 1967; Amthor and Oyster 1995). In flies, the four levels of T5 cell terminals representing four orientation-specific directional maps in the lobula plate suggest four directional categories for the collators. Although behavioral studies of *Drosophila* (reviewed by Hausen 1993) suggest as many as six, the present results demonstrate that four coarsely coding directional classes are sufficient to generate robust selectivity to complex multidirectional optic flows. Global motion-processing pathways in rabbits are supplied by only three directional classes of ON-direction selective ganglion cells (Vaney et al. 2000). Preliminary tests of this model, employing three SFMD arrays with preferred directions separated by 120°, produce results that are remarkably consistent with those of the four-subtype model. Additional recordings from direction-sensitive T5 cells (Douglass and Strausfeld 1995) and other small-field direction-sensitive inputs, such as Y-cells (Douglass and Strausfeld 1998) will determine how many preferred motion directions are available as inputs to wide-field collators. Because wide-field collator neurons are postsynaptic to T5 afferents from SFMDs, they offer an additional source of information regarding the distribution of preferred directions. The model predicts that imaging of spatial activity patterns in the dendrites of optic flow-sensitive neurons with voltage- or calcium-sensitive dyes, as has been pioneered by Single and Borst (1998), can unambiguously reveal the number of preferred directions.

Innervation matrices for non-centered flows

The innervation matrices used in this investigation are designed to generate selectivity for optic flow patterns that are centered on the receptive field of the collator neuron. In primate MSTd, certain neurons are selective for centered flows, while others prefer displaced flows (Duffy and Wurtz 1995). It is expected that recordings will identify both types of neurons among the ensembles of 60 or so wide-field tangential neurons in the lobula plate of various Diptera (see Hausen 1993; Strausfeld et al. 1995; Buschbeck and Strausfeld 1997). So far, the most complete physiological data concerning optic flow selectivity consist of spatial maps of local directional selectivity by dendritic branches of VS neurons that are sensitive to displaced flows (Krapp et al. 1998). The present model suggests how innervation matrices should be organized to generate selectivity for such flows. Predicted spatial patterns of SFMD activity depend on flow position, and show what regions of a collator receptive field contain SFMDs with the largest response amplitudes. For example Fig. 7 (R_A–R_D, position 1) reveals those regions where the strongest synaptic connections from SFMDs would be expected if a collator neuron is selective for clockwise flow with the COM lying at the left edge of the receptive field. Figure 11 suggests innervation matrices that should produce such selectivity if the small-field tuning is R_B-like, using either purely excitatory (Fig. 11A) or combined excitatory/inhibitory connections (Fig. 11B).

Small-field tuning versus wide-field innervation matrices

In keeping with the coarse coding properties of many sensory systems (Sparks et al. 1997), motion-sensitive neurons tend to be broadly tuned to the direction of motion, but the details of directional tuning vary among different systems. Directional tuning can be very narrow (e.g., Judge and Rind 1997), or quite broad, as in rabbit retinal ganglion cells (Oyster 1968) or in fly wide-field tangential neurons (Srinivasan and Dvorak 1980) and T5 neurons (Douglass and Strausfeld 1995). Responses may be purely excitatory, as in ON-OFF directionally

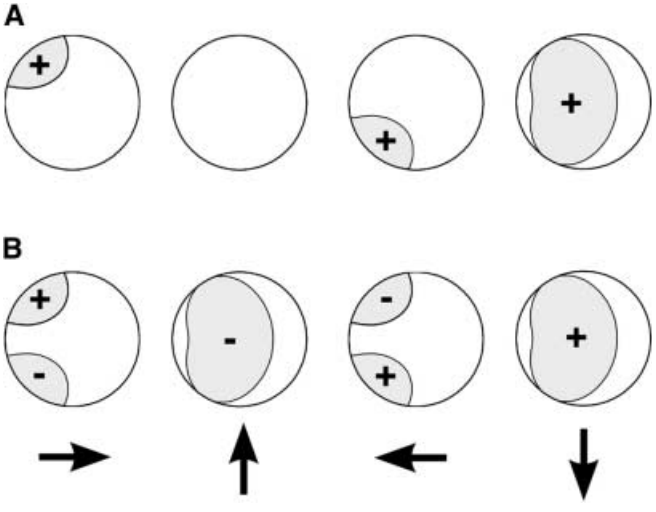

Fig. 11A, B Two sets of predicted innervation matrices for a clockwise rotatory flow field (center of motion located at the left edge of the collator receptive field) in a network whose small-field tuning matches function R_B. The first set (**A**) assumes uniform excitatory synaptic connections, while the second (**B**) employs both excitatory and inhibitory outputs (see Douglass and Strausfeld 2000a). The patterns are based on the predicted presynaptic activity of four arrays of small-field motion detectors that are broadly tuned to motion direction (*arrows* show the preferred direction for the corresponding arrays) and exhibit both excitatory and inhibitory activity (see Fig. 7, small field function R_B, position *1*). *Shaded areas* represent retinotopic regions in which small-field motion detectors would be presynaptic onto the dendrites of a wide-field collator

selective ganglion cells (Oyster 1968), or include inhibitory responses, as in T5 cells (Douglass and Strausfeld 1995).

In view of these observations, the sensitivity of the present model to small-field tuning is of some interest. In order to generate selectivity for a particular flow field (Fig. 4), it seems reasonable to suppose that the detailed response properties of small-field inputs are not critical as long as directional selectivity is present and the outputs are filtered through an appropriate wide-field innervation matrix. On the other hand, because directional information is crucial to the analysis of optic flow, it should be possible to optimize small-field tuning properties for use by subsequent processing levels. The present results support the latter view, as only one of four alternative small-field functions (R_B) produces strong selectivity for both flow type and position. These observations are also consistent with theoretical analyses suggesting that for a given sensory parameter, an optimal tuning curve bandwidth results in maximal information transfer to subsequent processing levels (Heiligenberg 1987; Theunissen and Miller 1991; Salinas and Abbott 1994).

Finally, it should be stressed that this model's sensitivity to small-field tuning has important functional implications for optimizing optic flow-processing in the fly lobula plate, and the extent to which vertebrates and invertebrates share similar mechanisms. Data from T5 neurons (Douglass and Strausfeld 1995) show directional tuning properties comparable to the most successful model small-field function, R_B. This suggests that flies may indeed be constrained to employ R_B-like tuning, and that optic flow selectivity could be compromised if those tuning properties are altered due to changes in stimulus conditions. Possibly, homeostatic mechanisms exist that can stabilize the tuning properties of T5 cells and other small-field directional motion-sensitive neurons. However, an alternative solution (Douglass and Strausfeld 2000a) involves changes to the wide-field innervation matrices which can dramatically reduce the dependence of collators on perturbable features of their small-field afferents.

Acknowledgements The development of this model has benefited from discussions with Dr. Charles M. Higgins. Dr. Mandyam V. Srinivasan provided helpful comments on an early version of the manuscript. Grant sponsors: AFOSR 980803 (to JKD); NIH NCRR 08688 and ONR N00014-97-1-0970 (to NJS).

References

Amthor FR, Oyster CW (1995) Spatial organization of retinal information about the direction of image motion. Proc Natl Acad Sci USA 92: 4002–4005

Beersma DGM, Stavenga DG, Kuiper JW (1977) Retinal lattice, visual field and binocularities in flies. J Comp Physiol 119: 207–220

Borst A (1991) Fly visual interneurons responsive to image expansion. Zool Jb Physiol 95: 305–313

Borst A, Egelhaaf M (1989) Principles of visual motion detection. Trends Neurosci 12: 297–306

Borst A, Egelhaaf M (1990) Direction selectivity of blowfly motion-sensitive neurons is computed in a two-stage process. Proc Natl Acad Sci USA 87: 9363–9367

Brotz TM, Borst A (1996) Cholinergic and GABAergic receptors on fly tangential cells and their role in visual motion detection. J Neurophysiol 76: 1786–1799

Buchner E (1976) Elementary movement detectors in an insect visual system. Biol Cybern 24: 85–101

Buchner E, Buchner S (1984) Neuroanatomical mapping of visually induced neuron activity in insects by 3H-deoxyglucose. In: Ali MA (ed) Photoreception and vision in invertebrates. Plenum Press, New York, pp 623–634

Buschbeck EK, Strausfeld NJ (1996) Visual motion detection circuits in flies: small-field retinotopic elements responding to motion are evolutionarily conserved across taxa. J Neurosci 16: 4563–4578

Buschbeck EK, Strausfeld NJ (1997) The relevance of neural architecture to visual performance: phylogenetic conservation and variation in dipteran visual systems. J Comp Neurol 383: 282–304

Collett TS, Land MF (1975). Visual control of flight behaviour in the hoverfly, *Syritta pipiens* L. J Comp Physiol A 99: 1–66

Cornilleau-Pérès V, Gielen CCAM (1996) Interactions between self-motion and depth perception in the processing of optic flow. Trends Neurosci 19: 196–202

David CT (1982) Compensation for height in the control of groundspeed by *Drosophila* in a new "Barber's Pole" wind tunnel. J Comp Physiol 147: 485–493

Douglass JK, Strausfeld NJ (1995) Visual motion detection circuits in flies: peripheral motion computation by identified small-field retinotopic neurons. J Neurosci 15: 5596–5611

Douglass JK, Strausfeld NJ (1996) Visual motion-detection circuits in flies: parallel direction- and non-direction-sensitive pathways between the medulla and lobula plate. J Neurosci 16: 4551–4562

Douglass JK, Strausfeld NJ (1998) Functionally and anatomically segregated visual pathways in the lobula complex of a calliphorid fly. J Comp Neurol 396: 84–104

Douglass JK, Strausfeld NJ (2000a) Optic flow representation in the optic lobes of Diptera: modeling collator innervation matrices onto collators and their evolutionary implications. J Comp Physiol A (in press) DOI 10.1007/s003590000132

Douglass JK, Strausfeld NJ (2000b) Pathways in dipteran insects for early visual motion processing. In: Zanker JM, Zeil J (eds) Motion vision: Computational, neural and ecological constraints. Springer, Berlin Heidelberg New York, pp 67–81

Duffy CJ, Wurtz RH (1991a) Sensitivity of MST neurons to optic flow stimuli. I. A continuum of response selectivity to large-field stimuli. J Neurophysiol 65: 1329–1345

Duffy CJ, Wurtz RH (1991b) Sensitivity of MST neurons to optic flow stimuli. II. Mechanisms of response selectivity revealed by small-field stimuli. J Neurophysiol 65: 1346–1359

Duffy CJ, Wurtz RH (1995) Response of monkey MST neurons to optic flow stimuli with shifted centers of motion. J Neurosci 15: 5192–5208

Farina WM, Varju D, Zhou Y (1994) The regulation of distance to dummy flowers during hovering flight in the hawk moth *Macroglossum stellatarum*. J Comp Physiol 174: 239–247

Fischbach K-F, Dittrich APM (1989) The optic lobe of *Drosophila melanogaster*. I. A Golgi analysis of wild-type structure. Cell Tissue Res 258: 441–475

Franceschini N, Riehle A, Le Nestour A (1989) Directionally selective motion detection by insect neurons. In: Stavenga DG, Hardie RC (eds) Facets of vision. Springer, Berlin Heidelberg New York, pp 360–390

Gabbiani F, Krapp HG, Laurent G (1999) Computation of object approach by a wide-field, motion-sensitive neuron. J Neurosci 19: 1122–1141

Gilbert C, Penisten DK, DeVoe RD (1991) Discrimination of visual motion from flicker by identified neurons in the medulla of the fleshfly *Sarcophaga bullata*. J Comp Physiol A 168: 653–673

Götz KG (1975) The optomotor equilibrium of the *Drosophila* navigation system. J Comp Physiol A 99: 187–210
Graziano MSA, Andersen RA, Snowden RJ (1994) Tuning of MST neurons to spiral motions. J Neurosci 14: 54–67
Gronenberg W, Strausfeld NJ (1990) Descending neurons supplying the neck and flight motor of Diptera: physiological and anatomical characteristics. J Comp Neurol 302: 973–991
Hassenstein B, Reichardt W (1956) Systemtheoretische Analyse der Zeit-, Reihenfolgen- und Vorzeichenauswertung bei der Bewegungsperzeption des Rüsselkäfers *Chlorophanus*. Z Naturforsch 11: 513–524
Hausen K (1982a) Motion sensitive interneurons in the optomotor system of the fly. I. The horizontal cells: structure and signals. Biol Cybern 45: 143–156
Hausen K (1982b) Motion sensitive interneurons in the optomotor system of the fly. II. The horizontal cells: receptive field organization and response characteristics. Biol Cybern 46: 67–79
Hausen K (1984) The lobula complex of the fly: structure, function and significance in visual behavior. In: Ali MA (ed) Photoreception and vision in invertebrates. Plenum, New York, pp 523–599
Hausen K (1993) Decoding of retinal image flow in insects. In: Miles FA, Wallman J (eds) Visual motion and its role in the stabilization of gaze. Elsevier, pp 203–235
Hausen K, Egelhaaf M (1989) Neural mechanisms of visual course control in insects. In: Stavenga GG, Hardie RC (eds) Facets of vision. Springer, Berlin Heidelberg New York, pp 391–424
Heiligenberg W (1987) Central processing of sensory information in electric fish. J Comp Physiol A 161: 621–631
Hengstenberg R (1982) Common visual response properties of giant vertical cells in the lobula plate of the blowfly *Calliphora erythrocephala*. J Comp Physiol A 149: 179–193
Holmqvist MH, Srinivasan MV (1991) A visually evoked escape response of the housefly. J Comp Physiol A 169: 451–459
Hubel DH, Wiesel TN (1962) Receptive fields, binocular interaction and functional architecture in the cat's visual cortex. J Physiol (Lond) 160: 106–154
Judge SJ, Rind FC (1997) The locust DCMD, a movement-detecting neurone tightly tuned to collision trajectories. J Exp Biol 200: 2209–2216
Kern R (1998) Visual position stabilization in the hummingbird hawk moth, *Macroglossum stellatarum* L. II. Electrophysiological analysis of neurons sensitive to wide-field motion. J Comp Physiol A 182: 239–249
Koenderink JJ (1986) Optic flow. Vision Res 26: 161–180
Krapp HG, Hengstenberg R (1996) Estimation of self-motion by optic flow processing in single visual interneurons. Nature (Lond) 384: 463–466
Krapp HG, Hengstenberg B, Hengstenberg R (1998) Dendritic structure and receptive-field organization of optic flow processing interneurons in the fly. J Neurophysiol 79: 1902–1917
Lappe M, Rauschecker JP (1993) A neural network for the processing of optic flow from ego-motion in man and higher mammals. Neural Comput 5: 374–391
Laughlin S (1981) Neural principles in the peripheral visual systems of invertebrates. In: Autrum H (ed) Comparative physiology and evolution of vision in invertebrates. In: Handbook of sensory physiology, vol VII/6B. Springer, Berlin Heidelberg New York, pp 133–280
Lewis JE, Kristan WB Jr (1998) Quantitative analysis of a directed behavior in the medicinal leech: implications for organizing motor output. J Neurosci 18: 1571–1582
Maunsell JHR, Van Essen DC (1983) Functional properties of neurons in middle temporal visual area of the macaque monkey. I. Selectivity for stimulus direction, speed, and orientation. J Neurophysiol 49: 1127–1147
Nakayama K (1985) Biological image motion processing: a review. Vision Res 25: 625–660
Olberg RM (1981) Parallel encoding of direction of wind, head, abdomen, and visual-pattern movement by single interneurons in the dragonfly. J Comp Physiol 142: 27–41
Oyster CW (1968) The analysis of image motion by the rabbit retina. J Physiol (Lond) 199: 613–635
Oyster CW, Barlow HB (1967) Direction-selective units in rabbit retina: distribution of preferred directions. Science 155: 841–842
Perrone JA (1992) Model for the computation of self-motion in biological systems. J Opt Soc Am A 9: 177–194
Perrone JA, Stone LS (1994) A model of self-motion estimation within primate extrastriate visual cortex. Vision Res 34: 2917–2938
Perrone JA, Stone LS (1998) Emulating the visual receptive-field properties of MST neurons with a template model of heading estimation. J Neurosci 18: 5958–5975
Rind C (1996) Intracellular characterization of neurons in the locust brain signaling impending collision. J Neurophysiol 75: 986–995
Rind FC, Bramwell DI (1996) Neural network based on the input organization of an identified neuron signaling impending collision. J Neurophysiol 75: 967–985
Saito H, Yukie M, Tanaka K, Hikosaka K, Fukada Y, Iwai E (1986) Integration of direction signals of image motion in the superior temporal sulcus of the macaque monkey. J Neurosci 6: 145–157
Salinas E, Abbott LF (1994) Vector reconstruction from firing rates. J Comput Neurosci 1: 89–107
Simpson JI, Graf W, Leonard C (1981) The coordinate system of visual climbing fibres to the flocculus. In: Fuchs AF, Becker W (eds) Progr Oculomotor Res, pp 475–484
Single S, Borst A (1998) Dendritic integration and its role in computing image velocity. Science 281: 1848–1850
Sparks DL, Kristan WB Jr, Shaw BK (1997) The role of population coding in the control of movement. In: Stein PSG, Grillner S, Selverston AI, Stuart DG (eds) Neurons, networks and motor behavior. MIT Press, Cambridge, Mass., pp 21–32
Srinivasan MV, Dvorak DR (1980) Spatial processing of visual information in the movement-detecting pathway of the fly. Characteristics and functional significance. J Comp Physiol 140: 1–23
Srinivasan MV, Lehrer M, Kirchner WH, Zhang SW (1991) Range perception through apparent image speed in freely flying honeybees. Visual Neurosci 6: 519–535
Strausfeld NJ (1976) Atlas of an insect brain. Springer, Berlin Heidelberg New York
Strausfeld NJ (1989) Beneath the compound eye: neuroanatomical analysis and physiological correlates in the study of insect vision. In: Stavenga DG, Hardie RC (eds) Facets of vision. Springer, Berlin Heidelberg New York, pp 317–359
Strausfeld NJ, Bassemir UK (1985) Lobula plate and ocellar interneurons converge onto a cluster of descending neurons leading to neck and leg neuropil in *Calliphora erythrocephala*. Cell Tissue Res 240: 617–640
Strausfeld NJ, Lee J-K (1991) Neuronal basis for parallel visual processing in the fly. Vis Neurosci 7: 13–33
Strausfeld NJ, Kong B, Milde JJ, Gilbert C, Ramaiah C (1995) Oculomotor control in calliphorid flies: neural organization in heterolateral inhibitory pathways. J Comp Neurol 361: 298–320
Sun H, Frost BJ (1998) Computation of different optical variables of looming objects in pigeon nucleus rotundus neurons. Nature Neurosci 1: 296–303
Tanaka K, Saito H (1989) Analysis of motion of the visual field by direction, expansion/contraction, and rotation cells clustered in the dorsal part of the medial superior temporal area of the macaque monkey. J Neurophysiol 62: 626–641
Theunissen FE, Miller JP (1991) Representation of sensory information in the cricket cercal sensory system. II. Information theoretic calculation of system accuracy and optimal tuning-curve widths of four primary interneurons. J Neurophysiol 66: 1690–1703
Vaney DI, He S, Taylor WR, Levick WR (2000) Direction-selective ganglion cells in the retina. In: Zanker JM, Zeil J (eds) Motion vision: Computational, neural and ecological constraints. Springer, Berlin Heidelberg New York pp. 13–56
Wagner H (1982) Flow-field variables trigger landing in flies. Nature (Lond) 297: 147–148
Wang YC, Frost BJ (1992) Time to collision is signaled by neurons in the nucleus rotundus of pigeons. Nature (Lond) 356: 236–238

Wicklein M, Strausfeld NJ (2000) Organization and significance of neurons that detect change of visual depth in the hawk moth *Manduca sexta*. J Comp Neurol 424: 356–376

Wyatt HR, Daw N (1975) Directionally sensitive ganglion cells in the rabbit retina: specificity for stimulus, direction, size, and speed. J Neurophysiol 38: 613–626

Wylie DRW, Frost BJ (1999a) Complex spike activity of Purkinje cells in the ventral uvula and nodulus of pigeons in response to translational optic flow. J Neurophysiol 81: 256–266

Wylie DRW, Frost BJ (1999b) Responses of neurons in the nucleus of the basal optic root to translational and rotational flowfields. J Neurophysiol 81: 267–276

Zaagman WH, Mastebroek HAK, Kuiper JW (1978) On the correlation model: performance of a movement detecting neural element in the fly visual system. Biol Cybern 31: 163–168

Zanker JM (1990) On the directional sensitivity of motion detectors. Biol Cybern 62: 177–183